Mono and Simultaneous Adsorption of Aldrin and Toxic Metals from Aqueous Solution Using Rice Husk Biochar

Tibamba Matthew Tichem,[a] Youbao Wang,[a,*] Raphael B. H. Gameli,[b] Bawa Mbage,[c] Abudu Ballu Duwiejuah,[d] Nannan Wang,[e] and Li Bing [f]

Recent research has explored the potential of rice husk biochar as a low-cost adsorbent for the removal of contaminants from aqueous solutions, including aldrin, mercury (Hg^{2+}), lead (Pb^{2+}), and cadmium (Cd^{2+}). Experimentation involved adding varying doses of biochar to wastewater with different contamination levels, agitating the mixture for 60 min, and filtering the solutions for analysis. The experiment revealed impressive removal efficiencies: 100% for aldrin, 99.92% - 99.99% for Hg^{2+}, 95.90% - 99.52% for Pb^{2+}, and 88.60% - 99.46% for Cd^{2+}. In binary and quaternary mixtures, Hg^{2+} showed higher removal efficiency than Pb^{2+} and Cd^{2+}, with the exception of aldrin. The adsorption order was identified as aldrin > Hg^{2+} > Pb^{2+} > Cd^{2+}. The Freundlich adsorption isotherm best described heavy metals in the mono and quaternary component adsorption, while the Langmuir adsorption isotherm was a better fit for the binary component. Consequently, the study highlights rice husk biochar as an efficient, sustainable, and environmentally friendly option for wastewater treatment.

DOI: 10.15376/biores.19.1.257-275

Keywords: Adsorption; Aldrin; Toxic metals; Biochar; Rice husk

*Contact information: a: School of Ecology and Environment, Anhui Normal University, No. 1 Beijing Donglu, Wuhu City, 241000, Anhui Province, China, ntilichemi@gmail.com; b: Department of Environmental Management and Sustainability Science, Faculty of Natural Resources and Environment, University for Development Studies, Post Office Box TL 1882, Tamale-Ghana, raphgameli@gmail.com; c: Department of Chemistry Education, University of Education, Winneba, Post Office Box 25, Winneba-Ghana, mbagebawa@yahoo.com; d: Department of Biotechnology and Molecular Biology, Faculty of Biosciences, University for Development Studies, Post Office Box TL 1882, Tamale-Ghana, aduwiejuah@uds.edu.gh; e: School of Ecology and Environment, Anhui Normal University, No. 1 Beijing Donglu, Wuhu City, 241000, Anhui Province, China, 174351691@qq.com; f: School of Ecology and Environment, Anhui Normal University, No. 1 Beijing Donglu, Wuhu City, 241000, Anhui Province, China, 1295469192@qq.com; *Corresponding author: wyb74@126.com*

INTRODUCTION

Water pollution is ever increasing and spreading. Such pollution has high mobility, which makes it a severe threat to both the environment and public health. The long-standing worry of the general public worldwide has been the efficient removal of contaminants from water. Toxic metals such as mercury (Hg^{2+}), lead (Pb^{2+}), cadmium (Cd^{2+}), and nickel (Ni) are becoming more prevalent as they make their way into water bodies such as groundwater aquifers, ponds, and rivers (Izah *et al.* 2016). These hazardous elements are introduced as a result of human activities related to development and modernisation. Toxic metals can impair or diminish brain and central nerve function, as well as affect energy levels and blood composition in people (Izah *et al.* 2016). Numerous investigations have revealed that herbicides have seriously contaminated surface water (Moschet *et al.* 2014) and

groundwater (Zhang *et al.* 2015). After entering the body, aldrin rapidly transforms into dieldrin and remains in adipose tissue for a considerable amount of time (Agency for toxic substances and disease registry (ATSDR 2002). High levels of exposure to aldrin and dieldrin have been linked to dysfunction in the immune system, endocrine glands, neurological system, and cardiovascular organs, as well as cancer (Kamel and Hoppin 2014).

There are several strategies for removing these harmful metals from wastewater. Some of these strategies include evaporation, ion-ion exchange, reverse osmosis, membrane-based, solvent extraction, destruction by catalytic moist air oxidation, photocatalytic oxidation, precipitation, membrane pervaporation, and adsorption (Hussain *et al.* 2018). However, because of high cost and low removal efficiency, these techniques on a large scale are not preferred. In order to be widely marketed as an efficient and viable treatment process, the process must meet economic and environmental requirements (Enaime *et al.* 2020). The high costs associated with wastewater treatment are often unaffordable for most poor African countries (Enaime *et al.* 2020). Over these techniques, biochar application has been gaining more attention (Li *et al.* 2023).

Adsorption is becoming more popular as a technology for cleaning water and wastewater, but selecting the right adsorbent is crucial. Adsorption is a potential approach for the removal of heavy metals from aqueous environments, especially when adsorbents are generated from lignocellulosic materials (Al Moharbi *et al.* 2020). Agricultural wastes such as rice husks have a promising potential to be turned into a medium for effective removal of toxic materials in the environment. Rice is the world's second most extensively produced crop, and it generates the most garbage (Nakhshiniev *et al.* 2014). The majority of rice growers now dispose of rice husks by piling and open burning, despite the fact that they have potential uses as value-added goods. These disposal techniques harm the environment and public health in addition to using land resources (Mohammadi *et al.* 2016). As a result, it is very desirable to dispose of the rice husk biomass safely. In the meantime, after thermochemical processing, rice husk's high carbon content makes it easier for it to be converted into energy-rich biochar (Li *et al.* 2023). The structure of rice husk consists of cellulose, hemicellulose, and lignin. Rice husk biochar is one of the many varieties of biochar that is highly desirable, since it is inexpensive and environmentally friendly, as it is derived from leftover rice husk (Sadeghi Afjeh *et al*. 2020). It has excellent qualities and a broad range of applications across multiple fields characterise rice husk biochar.

A large amount of waste is produced in the course of agro-industrial production, much of which is disposed of incorrectly. Agricultural waste for instance can pose significant environmental challenges such as water pollution, soil degradation, and greenhouse gas emissions (Adedibu 2023). Rice husk biochar is utilised for the adsorption of heavy metals and organic compounds in water because of its excellent stability, recyclability, and adsorption capacity (Narzari *et al.* 2015). According to Ahmad *et al.* (2014) and Sun *et al.* (2019), there are five main mechanisms for heavy metal adsorption on rice husk biochar: physical adsorption between metal ions and rice husk biochar; ion exchange between metals ions adsorbed on the rice husk biochar surface (*e.g.*, K^+, Na^+ and Mg^{2+}); complexation of metals ions with functional groups (*e.g.*, carboxyl, hydroxyl) on the rice husk biochar surface; electrostatic interaction between metals ions and the rice husk biochar surface; and coprecipitation between metals ions on the rice husk biochar surface. According to Sanka *et al.* (2020), rice husk biochar outperforms corncob biochar in its ability to adsorb lead, iron, and chromium from industrial effluent. From industrial

wastewater, rice husk biochar removed 90% of the lead and 65% of the chromium; in contrast, corncob biochar removed just 35% of the lead and 20% of the chromium. According to Amen *et al.* (2020), biochar made from agricultural waste has strong Pb^{2+} and Cd^{2+} adsorption capabilities. Pb^{2+} was absorbed by rice husk biochar at a level of 96.4% and Cd^{2+} was adsorbed at 94.7%. Also, Higashikawa *et al.* (2016) reported that sawdust biochar was not as effective as rice husk biochar at removing Cd^{2+} and Ni^{2+} from solutions. Thus, rice husk biochar may be more suitable than biochar produced from other agricultural wastes for adsorbing heavy metals in water.

Rice husk generation in Ghana is high, and it is one of the main residues amongst different agricultural residues that can be used for production of biochar. These leftovers can be used once more as biomass to make adsorbents, which are substances that take pollutants out of the environment. Following this, rice husk becomes a viable biomass option for making adsorbents. These wastes, however, can be used for other purposes that benefit mankind and ensures sustainability. In this perspective, the rice sector is tremendously significant. The use of cheaper and more readily available materials in different recycling processes can reduce overall recycling costs and increase recycling efficiency. When compared to other traditional processes, the adsorption process using biochar from readily available biomass feedstock from agricultural waste has been deemed the most cost-effective and efficient. With the aim of using novel, inexpensive adsorbents in the elimination and/or reduction of pesticides in soils and waterways, this study therefore examined mono and simultaneous adsorption of aldrin, mercury, lead, and cadmium onto biochars produced from rice husk collected from the farmlands in Ghana.

EXPERIMENTAL

Rice Husk Collection and Biochar Production

Rice husks were collected from rice farmers in Tamale Metropolis. The rice husk was thoroughly searched, and all foreign materials and biomass were removed. Rice husk biochar was produced at 500 ± 5 °C. This was done by placing the rice husk into a 20 cm silver bowl, which was put into a muffle furnace with temperature set at a 500 °C and pyrolysed under a limited oxygen condition for 60 min. This was repeated several times to obtain the desired 800 kg. The prepared biochar was then ground using a laboratory mortar and pestle and then sieved using a 2 mm sieve.

Preparation of Stock Solution for Simulated Wastewater

First, 1.68 g of cadmium chloride, 1.35 g of mercury chloride, and 1.60 g of lead nitrate were dissolved in deionised water to create stock solutions for the aqueous phase. These solutions had concentrations of 1000 mg/L. To determine the number of compounds containing 1 mg of each heavy metal, the molecular weights (g/mole) of $CdCl_2$ (183.32), $HgCl_2$ (271.50), and $Pb(NO_3)_2$ (331.21) were calculated and divided, respectively. In a 1000 mL volumetric flask, heavy metal solution mixtures were made. Stock solution of organochlorine (aldrin) in 1000 ppm was obtained from Ghana Standard Board laboratory and kept in an airtight glass container at cool temperature of 5 degrees Celsius. In order to obtain desired concentrations, serial dilutions were done to obtain maximum concentration limits of the leaching contaminants. Dilution of aldrin stock was done with the same formula. However, acetonitrile solution was used in place of distilled water to dilute aldrin to desired concentration. Acetonitrile was chosen as solvent because aldrin is not soluble

in water but soluble in acetonitrile.

Batch Adsorption Experiment

The experiment was carried out in batches of mono, binary, and quaternary component systems. The adsorption experiment for aldrin was done by pipetting 1.00 mg/L of aldrin from the prepared aldrin solution (1 mL of aldrin was pipetted into a beaker and 9 mL of acetonitrile was pipetted and added to it) into 1000 mL of deionised water in 1000 mL volumetric flask. The solution was corked and thoroughly agitated to achieve a uniform mixture. A volume of 100 mL of the solution was transferred into a conical flask containing accurately weighed rice husk biochar of 1 g (the initial pH of the solution was recorded). The same process was repeated for 5 g and 10 g of rice husk biochar dosages (Table 1). The mixture was placed on an orbital shaker and adjusted firmly using cotton to avoid breakage of conical flask and spillage of the solution. The solution on the orbital shaker was agitated for 60 min at 160 rpm. Agitation speed and contact time enhances the adsorptive removal rate of contaminants via the mass transfer resistance and improvement of adsorbate and adsorbent surface interaction (Duwiejuah 2017). The solution was then filtered using a Whatman's filter paper into a 35 mL sampling bottles.

Table 1. Maximum Contamination Limits of Pollutants at Varied Dosages in Aqueous Phase

Batch	Metal	Conc. 1 mg/L at 1 g of dosage	Conc. 3 mg/L at 5 g of dosage	Conc. 5 mg/L at 10 g of dosage
Mono	Aldrin	1.00	3.00	5.00
	Cd	1.00	3.00	5.00
	Hg	1.00	3.00	5.00
	Pb	1.00	3.00	5.00
Binary	Aldrin: Cd	1.00: 1.00	3.00: 3.00	5.00: 5.00
	Aldrin: Hg	1.00: 1.00	3.00: 3.00	5.00: 5.00
	Aldrin: Pb	1.00: 1.00	3.00: 3.00	5.00: 5.00
	Cd: Hg	1.00: 1.00	3.00: 3.00	5.00: 5.00
	Cd: Pb	1.00: 1.00	3.00: 3.00	5.00: 5.00
	Hg: Pb	1.00: 1.00	3.00: 3.00	5.00: 5.00
Quaternary	Aldrin:Cd:Hg:Pb	1.0: 1.0: 1.00: 1.0	3.0: 3.0: 3.0: 3.0	5.0: 5.0: 5.0: 5.0

Similar experiments, following the afore mentioned procedure, were used for the entire experiment (including binary and quaternary batches) which includes the use of iron-modified and unmodified rice husk biochar, at different dosages and corresponding contamination limits. A total of 33 elutes were obtained at the end of the experiment. All elutes were well filtered using Whatman's filter paper, into 35 mL sampling bottles and then transported to the Ghana Water Company Limited, Accra for analysis. The elutes were transported in an ice chest to the University of Ghana's Ecological Laboratory for analysis. The Perkin Elmer PIN Accle 900T Graphite Atomic Absorption Spectrophotometer (AAS) (Waltham, USA) was used to analyze cadmium, mercury, and lead.

Calculation for Adsorption Capacity Contaminants by Biochar

The equilibrium concentration of the adsorbent and the uptake of the toxic metal (Q_e) for each toxic metal at each adsorbent dosage was calculated using Eq. 1. In percentage, adsorption capacity was calculated by Eq. 2,

$$Q_e = \frac{C_i - C_f}{M} \times V \quad (1)$$

$$Q_e = \frac{(C_i - C_f)V}{M} \times 100 \quad (2)$$

where M is the dosage or amount of adsorbent, Q_e is the adsorption capacity, C_i is the initial concentration of contaminants, C_f is the final concentration of contaminants after adsorption, and V is the volume of the solution.

Adsorption Isotherm Models

Langmuir model

The Langmuir isotherm is used to determine and know the maximum removal or adsorption capacity as well as the type of interaction between the metals and the adsorbent. Below is the Langmuir isotherm formula in the linear form,

$$\frac{C_e}{Q_m} = \frac{1}{K_L Q_{max}} + \frac{C_e}{Q_{max}} \quad (3)$$

where Q_{max} (mg/g) is the maximum number of adsorbed molecules on the adsorbent surface at any given moment, K_L is the Langmuir constant (L/mg), and C_e is the concentration of the adsorbate at equilibrium (mg/g) (Kecili *et al.* 2018).

The separation factor, R_L, is used in this model. This makes it possible to more clearly identify the crucial aspects of the Langmuir adsorption isotherm model. Additionally, the constant has no dimensions. R_L is expressed as follows,

$$R_L = \frac{1}{1 + K_L C_o} \quad (4)$$

where C_o is the starting concentration of the adsorbate and K_L is the Langmuir constant (mg/g). The adsorption is said to be unfavorable when the R_L exceeds 1. According to Ayawei *et al.* (2017), when the R_L is 1, it is linear; when it is zero, it is irreversible; and when it is between 0 and 1, it is favorable.

Freundlich model

The Freundlich isotherm provides an expression that allows the exponentially distributed actives on heterogeneous adsorbent surfaces and their energies to be described (Ayawei *et al.* 2017). The standard Freundlich adsorption isotherm model is in Eq. 5,

$$Q_e = K_F C_e^{1/n} \quad (5)$$

where C_e is the equilibrium concentration of adsorbate (mg/L), Q_e is the amount of hazardous metal removed at equilibrium per gram of the adsorbent (mg/g), K_F is the Freundlich isotherm constant (mg/g), and $^1/_n$ is the adsorption intensity. The $^1/_n$ value demonstrates the relative distribution of energy as well as the heterogeneity of the adsorption sites. If $^1/_n$ equals 1, the adsorption is considered typical. According to Ayawei *et al.* (2017), co-operative adsorption occurs when $^1/_n > 1$, whilst two-phase partition that is independent of concentration occurs when $n = 1$.

RESULTS AND DISCUSSION

Fourier-Transform Infrared Spectroscopy (FTIR) and SEM Analysis

FTIR spectroscopy is a non-destructive technique that can be used to identify the functional groups present on the surface of a material. In an FTIR analysis of rice husk biochar, absorbance peaks can be observed at specific wavenumbers indicative of different functional groups, as shown in Fig. 1.

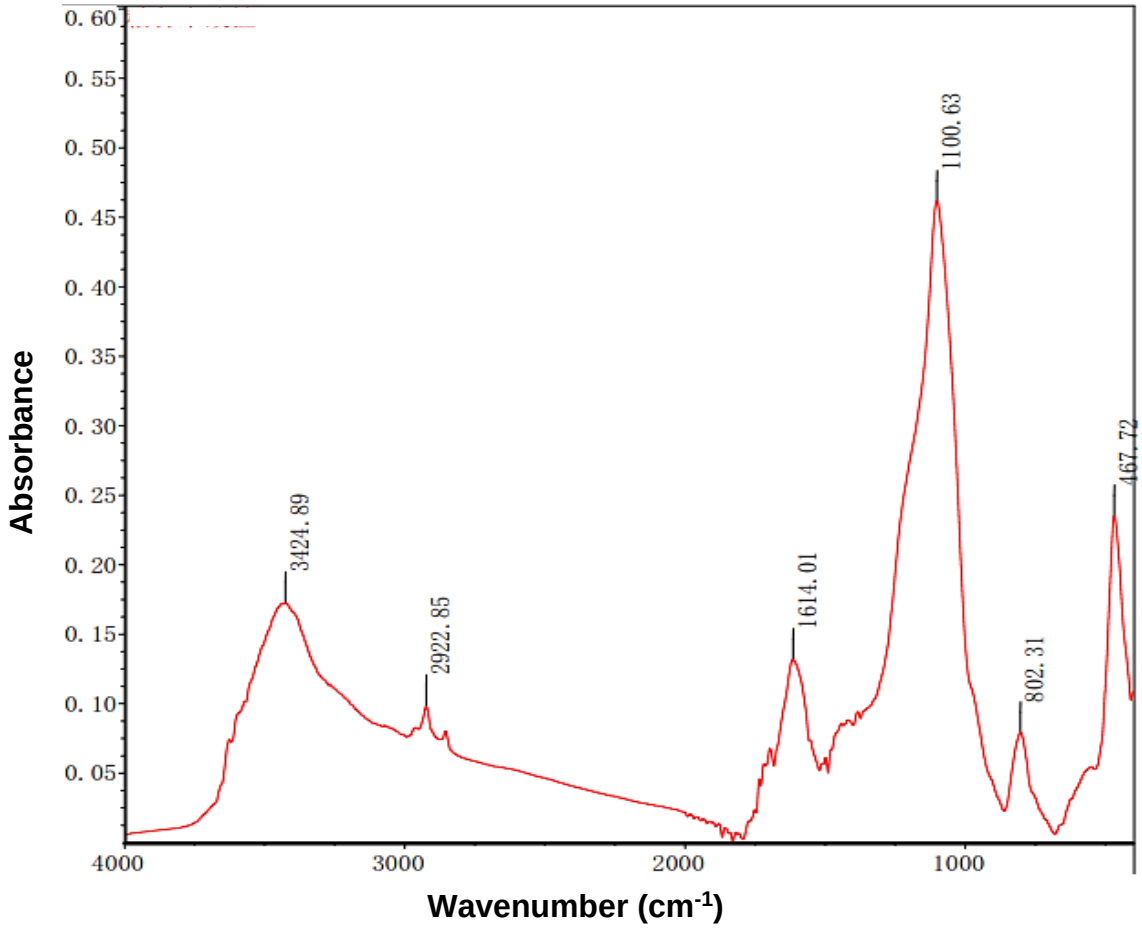

Fig. 1. FTIR analysis of rice husk biochar produced at 500 °C

A peak at 3424.9 cm^{-1} is typically due to O-H stretching vibrations, signifying the presence of hydroxyl groups or bonded water (Stuart 2004). Absorbance at 2922.8 cm^{-1} is commonly associated with C-H stretching in alkanes, suggesting the presence of -CH_2 or -CH_3 groups (Stuart 2004). A peak at 1614.0 cm^{-1} often corresponds to C=C stretching in aromatic compounds, while a peak at 1100.6 cm^{-1} indicates C-O stretching, possibly due to ether or alcohol groups (Silverstein *et al.* 2005). An absorbance peak at 802.3 cm^{-1} can represent out-of-plane bending of C-H bonds in aromatic compounds or Si-O structures (Silverstein *et al.* 2005). Lastly, a peak at 467.7 cm^{-1} often corresponds to metal-oxygen bonds or molecular rocking or wagging motions (Smith 2011). These interpretations are general, and exact functional groups should be identified considering the composition of the specific biochar and compared with reference spectra (Stuart 2004; Smith 2011).

Rice husk biochar produced at 500 °C, the SEM analysis showed a porous structure. The porosity is a result of the pyrolysis process, where volatile components are burned off, leaving a carbon-rich structure with voids where these components used to be (Nguyen *et al.* 2022). The surface of rice husk biochar is typically rough and irregular due to these pores. The size and distribution of the pores comprises a mixture of micro and macro pores. The micro pores are less than 2 nm in size, while the macro pores are larger. The specific morphology and porosity of the rice husk biochar can significantly impact its functionality, such as its adsorption capacity. A more porous structure generally leads to a higher surface area, which can enhance the biochar adsorption capacity. The SEM images depicts plant's cellular structure, appearing as bright spots in SEM images due to their higher electron density.

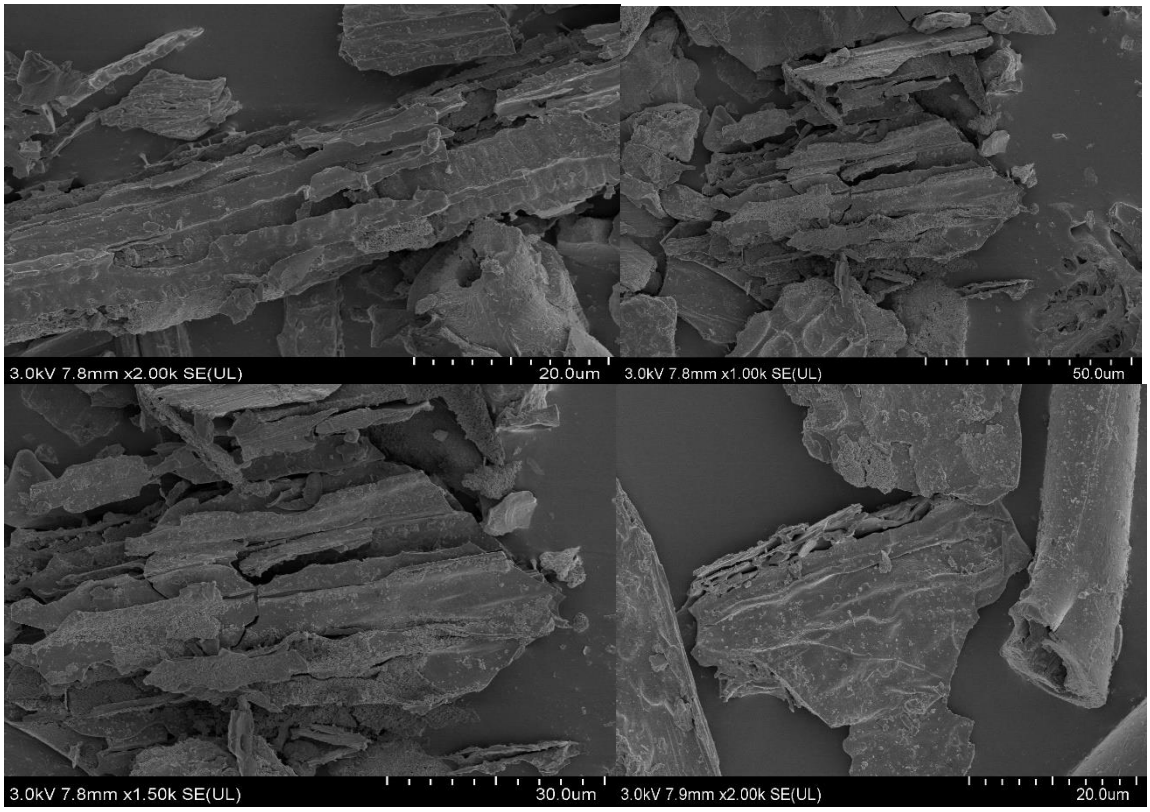

Fig. 2. SEM analysis of rice husk biochar produced at 500 °C

Adsorption Efficiency of Mono Metals onto Rice Husk Biochar

The adsorption efficiency of mercury in the mono component ranged from 99.92% to 99.99% as indicated in Table 2. The adsorption efficiency of mercury onto rice husk biochar increased as the adsorbent dosage was increased along with an increase in contaminant limits. Similar outcome was also recorded for Pb and Cd. These observed increases in adsorption efficiency when adsorbent dosage increases could be attributed to the availability of more active sites for the metal ions to bind.

The adsorption efficiency of Hg^{2+} onto the biochar was considerably higher than Pb^{2+} and Cd^{2+}. This occurrence could be attributed to the fact that Hg^{2+} has higher and stronger affinity to the rice husk biochar active site and surface energies as well as the functional groups in the organic matter, including phenolic and carboxylic groups. This outcome is consistent with the outcome reported by Park *et al.* (2019).

The adsorption efficiency of aldrin was 100% throughout the study (Table 2). The complete adsorption of aldrin in the mono component could be a result of the nature of rice husk. Rice husk biochar has a huge surface area and porous structure, which makes it an efficient adsorbent for contaminants in water. Because of the enormous surface area of biochar, contaminants can bind to it, boosting the overall adsorption capacity. Similar findings were reported by Malik *et al.* (2017) and Cara *et al.* (2022).

Table 2. Mono Component Adsorption of Pollutants in Aqueous Solution

Pollutant	Dosage (g)	pH	Initial Conc. (mg/L)	Final Conc. (mg/L)	Removal Efficiency (%)
Hg^{2+}	1	7.34	1	0.00079	99.92
	5	7.26	3	0.00041	99.99
	10	7.35	5	0.00029	99.99
Pb^{2+}	1	7.45	1	0.041	95.90
	5	7.47	3	0.026	99.13
	10	7.51	5	0.024	99.52
Cd^{2+}	1	7.67	1	0.114	88.60
	5	7.64	3	0.022	99.27
	10	7.65	5	0.027	99.46
Aldrin	1	7.04	1	0	100
	5	7.23	3	0	100
	10	7.14	5	0	100

Adsorption of Contaminant in Binary and Quaternary Components

The removal efficiency of Hg^{2+} and Pb^{2+} in a binary component increased with increasing adsorbent dosage (Table 3). This is due to the availability of more active sites for metal ions to bind to, boosting adsorption effectiveness. In all combinations, the removal efficiency of Hg^{2+} was higher than that of Pb^{2+} and Cd^{2+}. Mercury had a higher charge density than cadmium, forming strong bonds with the adsorbent, leading to a higher removal efficiency. Additionally, mercury had a higher electronegativity than cadmium, which indicates a greater tendency to attract electrons.

Aldrin had a 100% removal efficiency at all adsorbent doses in the binary components (Table 3). The presence of functional groups including -OH, lignin, talins and -COOH in rice husk, which have a high affinity for organochlorine compounds, results in strong organochlorine adsorption by rice husk biochar (Bielská *et al.* 2018). These functional groups have a high adsorption capacity because they may establish hydrogen bonds with organochlorine molecules. Also, the presence of hemicellulose, cellulose, lignin and mineral ash in rice husk contributes to the removal of contaminants (Satbaev *et al.* 2021).

Effect of Pyrolysis Temperature

Pyrolysis temperature is an important parameter in the production of rice husk biochar, as it affects the physical and chemical properties of the resulting biochar, and it can have a significant impact on its potential applications. The pyrolysis temperature used in this study was 500 °C, and the biochar produced at this temperature had a good amount of porous surfaces that aided in the adsorption of toxic metals and other contaminants. The higher adsorption efficiency recorded in this study could be attributed to the temperature at which the biochar was produced.

Table 3. Binary and Quaternary Adsorption of Pollutants From Aqueous Solution

Binary Component	Pollutant	Dosage	pH	Initial Conc.	Final Conc.	Percentage (%)
Hg^{2+} -Pb^{2+}	Hg^{2+}	1	7.85	1	0.0021	99.79
		5	7.92	3	0.0024	99.92
		10	7.95	5	0.002	99.96
	Pb^{2+}	1	7.85	1	0.023	97.70
		5	7.92	3	0.026	99.13
		10	7.95	5	0.029	99.42
Hg^{2+} - Cd^{2+}	Hg^{2+}	1	7.96	1	0.00119	99.88
		5	7.97	3	0.00124	99.96
		10	8.01	5	0.00166	99.97
	Cd^{2+}	1	7.96	1	0.144	85.60
		5	7.97	3	0.111	96.30
		10	8.01	5	0.066	98.68
Pb^{2+} - Cd^{2+}	Pb^{2+}	1	8.07	1	0.069	93.10
		5	8.1	3	0.096	96.80
		10	8.15	5	0.032	99.36
	Cd^{2+}	1	8.07	1	0.039	96.10
		5	8.1	3	0.021	99.30
		10	8.15	5	0.018	99.64
Aldrin- Hg^{2+}	Aldrin	1	7.47	1	0	100.00
		5	7.14	3	0	100.00
		10	7.35	5	0	100.00
	Hg^{2+}	1	7.47	1	0.00029	99.97
		5	7.14	3	0.0023	99.92
		10	7.35	5	0.00016	100.00
Aldrin- Pb^{2+}	Aldrin	1	7.17	1	0	100.00
		5	7.12	3	0	100.00
		10	6.35	5	0	100.00
	Pb^{2+}	1	7.17	1	0.137	86.30
		5	7.12	3	0.015	99.50
		10	6.35	5	0.013	99.74
Aldrin- Cd^{2+}	Aldrin	1	6.47	1	0	100.00
		5	6.34	3	0	100.00
		10	7.11	5	0	100.00
	Cd^{2+}	1	6.47	1	0.019	98.10
		5	6.34	3	0.013	99.57
		10	7.11	5	0.014	99.72
Quaternary Component						
Aldrin- Hg^{2+} - Pb^{2+} - Cd^{2+}	Aldrin	1	6.91	1	0	100.00
		5	6.83	3	0	100.00
		10	6.52	5	0	100.00
	Hg^{2+}	1	6.91	1	0.0024	99.76
		5	6.83	3	0.0019	99.94
		10	6.52	5	0.0021	99.96
	Pb^{2+}	1	6.91	1	0.033	96.70
		5	6.83	3	0.026	99.13
		10	6.52	5	0.029	99.42
	Cd^{2+}	1	6.91	1	0.022	97.80
		5	6.83	3	0.016	99.47
		10	6.52	5	0.011	99.78

The porosity and specific surface area of rice husk biochar in a certain temperature range increases with increasing temperature of pyrolysis. This is presumably related to the formation of micropores and the decomposition of organic matter (Rajapaksha *et al.* 2015). Paethanom and Yoshikawa (2012) observed that pores were created during rice husk pyrolysis. These pores led to a sharp increase in the biochar specific surface area, but this porosity declined at temperatures above 600 °C. The rice husk biochar aromaticity upsurged with the increase in temperature of pyrolysis (Abrishamkesh *et al.* 2015). Also, high pyrolysis temperatures favour the basic functional groups generation. This is because as the temperature of pyrolysis increases, hemicellulose cellulose and start to degrade and some functional groups (*e.g.*, carboxyl, alcohol, chromene, lactone, quinine, *etc.*) are generated (Li *et al.* 2023).

Effect of Contact Time

The effect of contact time also plays a significant role in the adsorption of contaminants in an aqueous phase or solution. The contact time affects the amount of adsorbate that is removed from the solution and the rate at which this occurs. The present study made use of 60 min of contact time. This contact time allowed for the effective binding of the contaminants on the surface of the adsorbent. Similar outcome was reported by Zhang *et al.* (2019). A similar study by Abd El-Aziz *et al.* (2022) reported the effects of contact time on Cr^{3+} and Pb^{2+} removal. The removal of 75% for Cr^{3+} and 92% for Pb^{2+} were obtained at an equilibrium of 90 min. Generally, with increasing contact time, the percentage removal will be increased.

Effect of pH

The effect of pH on adsorption is heavily influenced by the kind of biochar and the target metal ion. The pH recorded throughout the study ranged from slightly acidic (6.34) to slightly basic (8.15). Biochar has a variety of surface functional groups, most of which are oxygen groups. The pH recorded in this study was slightly acidic in the quaternary component, ranging from 6.52 to 6.91. In the binary component, the pH was slightly basic, ranging from 6.34 to 8.15. The pH range for toxic metals in the mono component ranged from 7.04 to 7.67. Increasing the pH causes precipitation of insoluble hydrated oxide or hydroxide, lowering the availability of heavy metal ions for sorption. A fall in pH leads to an increase in hydrogen ion concentration and hence possible competition for the binding sites. In general, sorption media pH is connected to the metal adsorption mechanism of the surfaces from water and disclosed the nature of the physico-chemical interaction of metal ions in solution and the nature of the sorption sites. These results find support from a study by Li *et al.* (2019) and Ahmed and Ahmed (2019).

The highly critical factor regulating heavy metal adsorption is pH. Contrasts in pH straightforwardly influence the serious capacity of hydrogen ions with heavy metal ions at the dynamic binding sites on the biosorbent surface (Zhang *et al.* 2014). The influence of pH on Cr^{3+} and Pb^{2+} adsorption was studied in the pH range of 2 to 8 by Abd El-Aziz *et al.* (2022). The study showed that Cr^{3+} and Pb^{2+} adsorption performance improved as the pH value increased from pH 4 to 5. The highest adsorption efficiencies for Cr^{3+} and Pb^{2+} were found at pH 6, 63.2% and 40.1% for Cr^{3+} and Pb^{2+}, respectively. Then, the highest uptake, Cr^{3+} was at 0.62 mg/g whilst for Pb^{2+} was at 0.70 mg/g, and at pH 7 to 8, the uptake capacity for Cr^{3+} and Pb^{2+} decreased. At low pH the adsorbent surface is protonated, acting as a positive charge resulting in low uptake capacity (Tay *et al.* 2012). When pH is elevated, the binding sites on the adsorbent's surface deprotonate resulting in the reinforcement of

charge attraction (Sathasivam *et al.* 2010).

Adsorption Isotherm

Langmuir adsorption isotherm

The Langmuir isotherm is a popular model for describing molecule or ion adsorption on a solid surface. In the mono-component experiment, Hg had a maximum adsorption capacity (Q_{max}) of 256 mg/g, which was the highest among all the metal contaminants. Venkatesan *et al*. (2020) reported findings that agree favorably with the findings of this study in relation to the efficacy and the potency of rice husk biochar for the removal of toxic metals. Mercury's K_l value of 1.28×10^{-03} L/mg indicates that it is easily transferred from the solid phase to the liquid phase. The R_l value of Hg (1.00×10^{0}) (Table 5) indicates that the analysis of Hg^{2+} is linear, indicating that the adsorption is neither favorable nor unfavorable, and that the adsorbate has an equal affinity for the surface and the solution (Ayawei *et al.* 2017). The coefficient of determination (R^2) value of Hg was 0.92, which indicates a good fit of the metal analysis to the Langmuir model, and a highly accurate analysis. The K_L value of lead was -2.17 x 10^{-01} L/mg, which indicates that Pb^{2+} is not easily transferred from the solid phase to the liquid phase. Its coefficient of determination value of 0.51 indicates a moderate fit of the metal analysis to the model, and a somewhat accurate analysis. The mono-component of Cd^{2+} had a maximum adsorption capacity (Q_{max}) of 108 mg/g, and its K_L value of 2.15 x 10^{-02} L/mg indicates that Cd^{2+} is easily transferred from the solid phase to the liquid phase. Its R_L value of 1.11 x 10^{-00} indicates that the adsorption process is somewhat unfavorable, but that it still occurs. The cadmium coefficient of determination value of 0.98 indicates a good fit of the metal analysis to the model, and a highly accurate analysis.

Table 5. Adsorption Isotherm Parameters Based on Langmuir Adsorption Isotherm Model

Metal Ions	Q_{max} (mg/g)	K_L (l/ mg)	R_L	R^2
Hg	256.41	1.28×10^{-03}	$1.00 \times 10^{+00}$	0.923
Pb	-434.78	-2.17×10^{-01}	3.48×10^{-01}	0.5107
Cd	107.53	2.15×10^{-02}	$1.11 \times 10^{+00}$	0.983
Hg*- Pb	68.49	1.37×10^{-04}	$1.00 \times 10^{+00}$	0.0773
Hg- Pb*	17.24	-1.90×10^{-02}	9.43×10^{-01}	0.9916
Hg*- Cd	25.45	-7.63×10^{-04}	9.96×10^{-01}	0.8983
Hg- Cd*	204.08	2.24×10^{-01}	$1.22 \times 10^{+00}$	0.4313
Pb*- Cd	66.67	2.00×10^{-03}	$1.01 \times 10^{+00}$	0.7477
Pb- Cd*	416.67	1.25×10^{-01}	$1.63 \times 10^{+00}$	0.9196
Al- Hg*	58.82	-4.12×10^{-05}	$1.00 \times 10^{+00}$	0.9962
Al- Pb*	61.73	1.85×10^{-03}	$1.01 \times 10^{+00}$	0.9997
Al- Cd*	-120.48	-4.82×10^{-02}	7.59×10^{-01}	0.3533
Al- Hg*- Pb-Cd	-53.19	-3.72×10^{-03}	9.96×10^{-01}	0.2749
Al- Hg- Pb*- Cd	-61.72	-5.56×10^{-02}	8.33×10^{-01}	0.2184
Al- Hg- Pb-Cd*	5000	$1.00 \times 10^{+00}$	$6.00 \times 10^{+00}$	0.0011

In the Hg^{2+} - Cd^{2+} binary combination, Hg^{2+} had a Q_{max} value of 25.4 mg/g and a K_L value of -7.63 x 10^{-04} L/mg. The R_L value was 9.96 × 10^{-01} and the R^2 value was 0.8983. This indicates a good fit to the Langmuir adsorption isotherm. Also, the R_L value indicates that the adsorption was favourable. The R_l value for Cd^{2+} in this binary composition was 1.22 × 10^{00} which indicates unfavourable adsorption. This outcome is as a result of the ionic strength of the solution. Also, the R^2 obtained for cadmium was 0.4313, indicating a relatively poor fit to the Langmuir adsorption isotherm model. In the binary combination of Pb^{2+} - Cd^{2+}, the Pb^{2+} maximum adsorption capacity Q_{max} value was 66.7 mg/g and a K_L value of 2.00 × 10^{-03} L/mg. The R_L value was 1.01 × 10^{-00} and the R^2 value was 0.7477 (Table 5). This indicates a good fit to the Langmuir adsorption isotherm. On the other hand, Cd^{2+} had higher maximum adsorption capacity of 417 mg/g and R^2 of 0.9196, indicating a better fit to the Langmuir adsorption model as compared to the lead. In the binary composition with aldrin, Hg^{2+}, Pb^{2+}, and Cd^{2+} had an R^2 of 0.9962, 0.9997, and 0.3533, respectively. This implies that Hg^{2+} and Pb^{2+} fit the Langmuir adsorption isotherm better than Cd^{2+}. This occurrence could be ascribed to factors that may be influencing the adsorption process. This could be the reason why cadmium had a lower R^2 in binary component with aldrin. Thus, the presence of other contaminants or competing adsorbate in the solution can impact the adsorption process by occupying adsorption sites or altering the surface chemistry of the adsorbent (Bakkaloglu *et al.* 2021).

In the quaternary combination Al - Hg^{2+} - Pb^{2+} - Cd^{2+}, the Q_{max} value obtained for Hg^{2+} was -53.19 mg/g and the K_L value was -3.72×10^{-03} L/mg. The R_L value was 9.96 × 10^{-01}, which means that the adsorption process was favourable. The R^2 value recorded for Hg^{2+} in the ternary component was 0.2749 (Table 5). This indicates a poor fit to the Langmuir adsorption isotherm. Also, the results obtained for Cd^{2+} and Pb^{2+} showed poor fits to the Langmuir adsorption isotherm. This occurrence could be as a result of the presence of other competing contaminants in the aqueous solution.

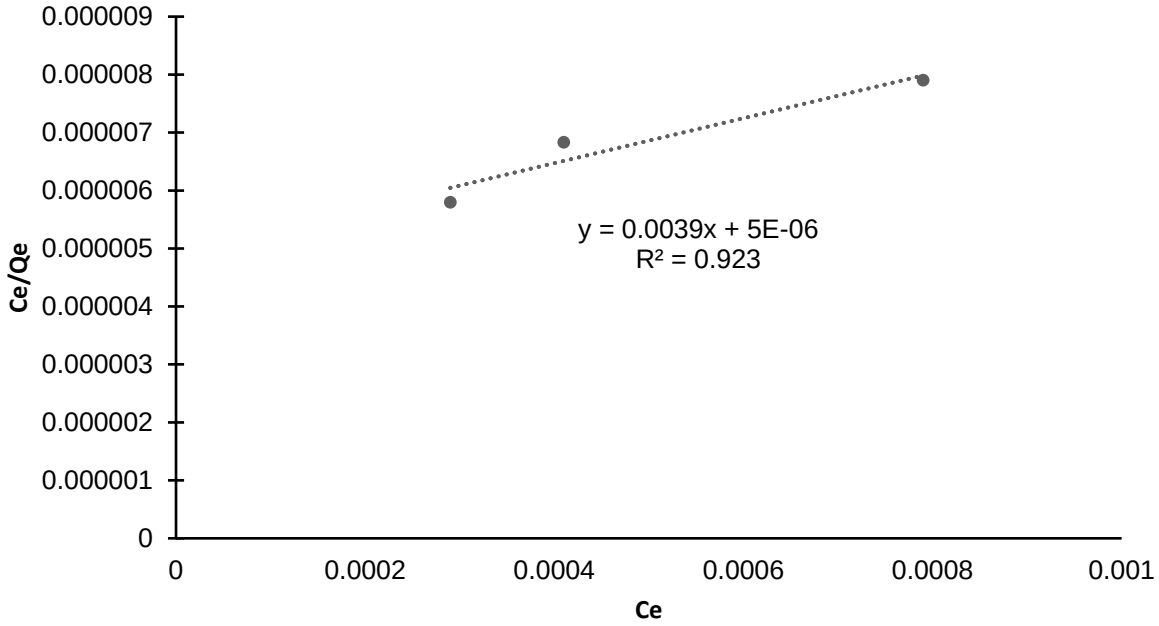

Fig. 3. Langmuir isotherm graph for the mono component adsorption of Hg^{2+} onto rice husk biochar which was produced at a temperature of 500 ± 5 °C (fast pyrolysis)

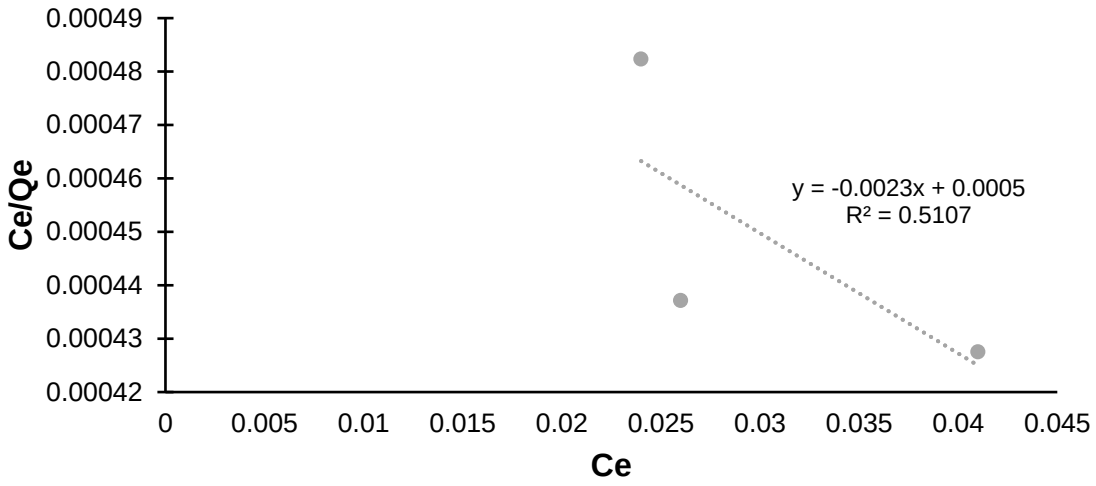

Fig. 4. Langmuir isotherm graph for the mono component adsorption of Pb^{2+} onto rice husk biochar which was produced at a temperature of 500 ± 5 ˚C (fast pyrolysis)

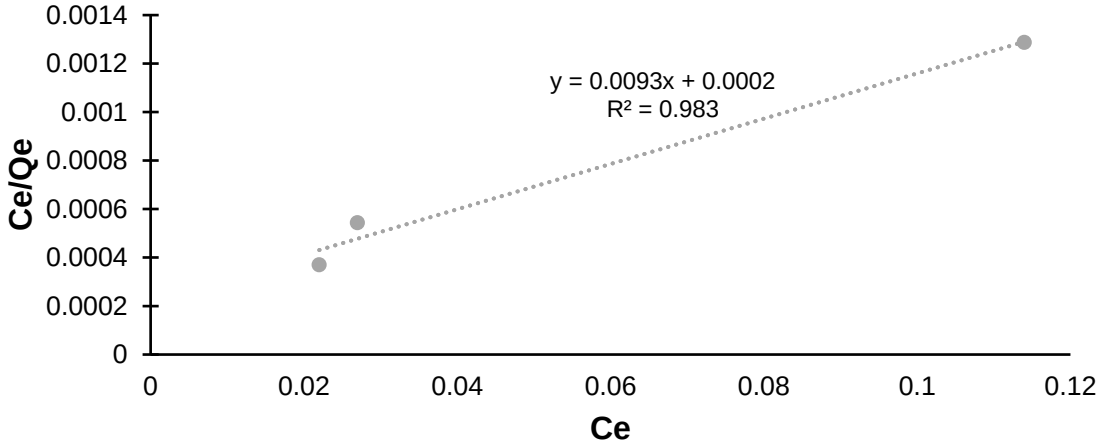

Fig. 5. Langmuir isotherm graph for the mono component adsorption of Cd^{2+} onto rice husk biochar which was produced at a temperature of 500 ± 5 ˚C (fast pyrolysis)

Freundlich isotherm

The Freundlich isotherm implies non-specific adsorption and a heterogeneous adsorbent surface with variable affinities for the solute (Freundlich 1906). Table 6 below represents adsorption data for pesticide (aldrin) and heavy metals (Hg^{2+}, Pb^{2+}, and Cd^{2+}), and the interaction between them in mono, binary, and quaternary systems. In the mono-component system, Hg^{2+} had the highest $^{1}/_{n}$ value of 1.42, indicating that its adsorption follows an S-type isotherm. Hg^{2+} had the highest K_F value of 14900 within the mono-component. A large value of K_F suggests that the adsorbent is a good candidate for the removal of the solute from a solution. Lead (Pb^{2+}) had a $^{1}/_{n}$ value of 0.86, indicating an L-type isotherm, which implies that the adsorption was favorable (Fatombi *et al.* 2019). Cd^{2+} had a $^{1}/_{n}$ value of 3.33, indicating a highly curved isotherm. This is due to a saturation of accessible adsorption sites for the chemical, resulting in reduced adsorption as concentration increases (Fatombi *et al.* 2019). In all the binary components, the Freundlich adsorption isotherm fitted Cd^{2+} in the binary component of Pb-Cd, the most. In the quaternary component, all three combinations of contaminants had $^{1}/_{n}$ values less than 1,

indicating L-type isotherms. This means that the adsorption process was favorable, and the adsorbate was relatively easily adsorbed onto the surface of the adsorbent.

The K_F value for Al- Hg*- Pb-Cd was the highest among all systems, which suggests that the adsorbent has a high capacity for adsorbing multiple heavy metals simultaneously. The R^2 value for Cd^{2+} was higher than Hg^{2+} and Pb^{2+}, indicating that the Freundlich adsorption isotherm fitted Cd^{2+} better than the other contaminants in the quaternary component system. These results are consistent with the study conducted by Chen *et al.* (2020).

Table 6. Freundlich Adsorption Isotherm Model of Contaminants

System	Pollutant	$^1/_n$	N	K_F (mg/g)	R^2
Mono	Hg^{2+}	1.42	0.70	14890.18	0.9918
	Pb^{2+}	0.86	1.16	3988.41	0.9839
	Cd^{2+}	3.33	0.30	167.38	0.8303
Binary	Hg^{2+*} -Pb^{2+}	-47.17	-0.02	58.71	3.00×10^{-05}
	Hg^{2+}- Pb^{2+*}	-0.34	-2.94	0.00	0.9476
	Hg^{2+*} - Cd^{2+}	-0.65	-1.54	0.00	0.6077
	Hg^{2+} - Cd^{2+*}	1.54	0.65	275.17	0.8252
	Pb^{2+*} - Cd^{2+}	3.83	0.26	134.87	0.2031
	Pb^{2+} - Cd^{2+*}	1.21	0.83	1416.12	0.9941
	Al - Hg^{2+*}	-71.94	-0.01	60.19	0.0029
	Al- Pb^{2+*}	6.29	0.16	107.32	0.9004
	Al- Cd^{2+*}	0.64	1.57	48150.41	0.8138
Quaternary	Al -Hg^{2+*}-Pb^{2+}-Cd^{2+}	0.43	2.34	121255096.1	0.5868
	Al – Hg^{2+}-Pb^{2+*}- Cd^{2+}	0.47	2.13	123452.53	0.5465
	Al- Hg^{2+}- Pb^{2+}- Cd^{2+*}	1.05	0.96	3526.14	0.9066

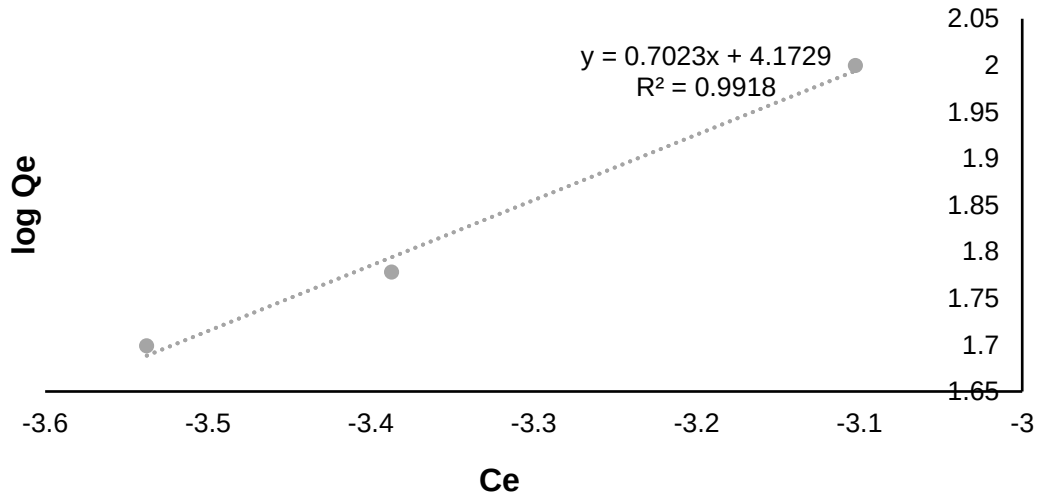

Fig. 6. Freundlich isotherm graph for the mono-component adsorption of Hg^{2+} onto rice husk biochar produced at a temperature of 500 ± 5 °C (fast pyrolysis)

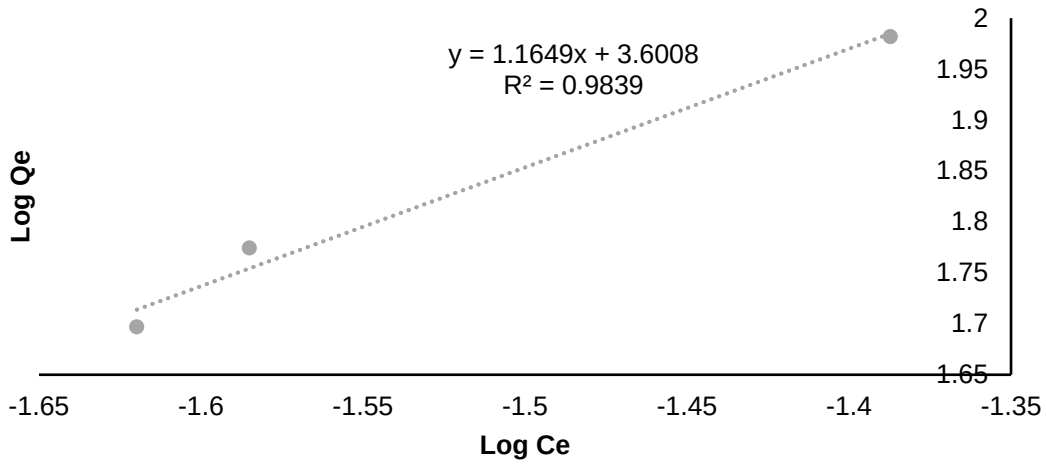

Fig. 7. Freundlich isotherm graph for the mono-component adsorption of Pb^{2+} onto rice husk biochar which was produced at a temperature of 500 ± 5 °C (fast pyrolysis)

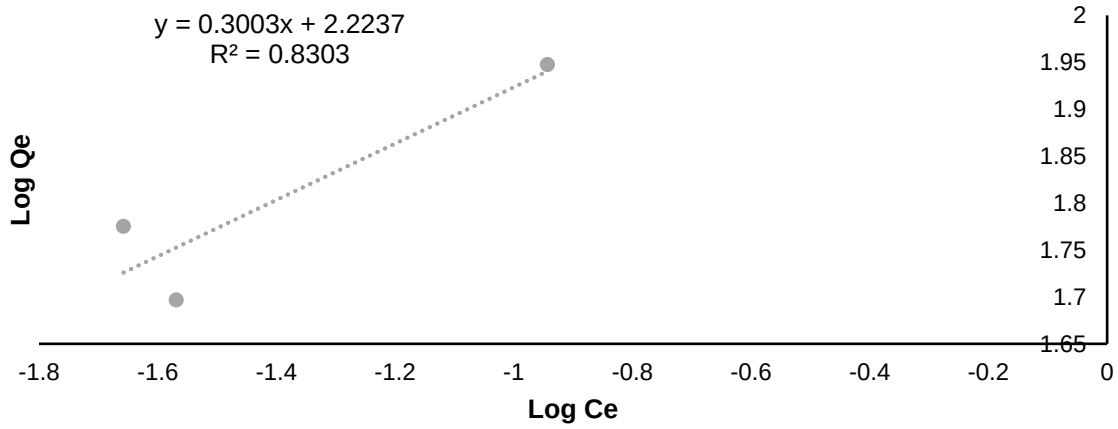

Fig. 8. Freundlich isotherm graph for the mono-component adsorption of Cd^{2+} onto rice husk biochar which was produced at a temperature of 500 ± 5 °C (fast pyrolysis)

CONCLUSIONS

1. In an FTIR analysis of rice husk biochar, absorbance peaks can be observed at specific wavenumbers indicative of different functional groups. For rice husk biochar produced at 500 °C, the SEM analysis showed a porous structure. The specific morphology and porosity of the rice husk biochar can significantly impact its functionality, such as its adsorption capacity. A more porous structure generally leads to a higher surface area, which can enhance the biochar adsorption capacity. The SEM images depicted the plant's cellular structure, appearing as bright spots in SEM images due to their higher electron density.
2. The efficiency of removing Hg^{2+}, Pb^{2+}, and Cd^{2+} using rice husk biochar in all component systems was high, ranging from 85.60% to 99.99%. The adsorption efficiency of mercury in the mono component ranged from 99.92% to 99.99%. The adsorption efficiency of mercury onto rice husk biochar increased as the adsorbent

dosage was increased along with an increase in contaminant limits. The adsorption efficiency of aldrin was 100% throughout the study. The complete adsorption of aldrin in the mono component could be as a result of the nature of rice husk. Rice husk biochar has huge surface area and porous structure make it an efficient adsorbent for contaminants in water. Aldrin was completely adsorbed due to the huge surface area and porous structure of rice husk biochar.

3. The pH of the solution affected the electrostatic attraction between metal ions and biochar, and the Freundlich and Langmuir adsorption isotherms were used to describe the type of adsorption. Adsorption efficiency of aldrin, mercury, lead and cadmium onto rice husk biochar increased as the adsorbent dosage was increased along with an increase in contaminant limits.

ACKNOWLEDGEMENT

We thank the University Synergy innovation Program of Anhui Province (GXXT-2020-075). This work was also supported by the Spanish Laboratory, University for Development Studies, Nyankpala Campus, Ghana, Ecological Laboratory of the University of Ghana and Ghana Standard Authority.

Data Availability

Data supporting the findings of this study are available from the corresponding author upon reasonable request.

Conflicts of Interest

There are no conflicts to declare.

REFERENCES CITED

Abd El-Aziz, M. S. M., Al-Masry, R. A., Hefnawy, H. T., and Khali, A. O. M. (2022). "Removal of Pb^{2+} and Cr^{3+} using rice husk as biosorbent," *Zagazig J. Agric. Res.* 49(5), 653-666. DOI: 10.21608/zjar.2022.269607

Abrishamkesh, S., Gorji, M., Asadi, H., Bagheri-Marandi, G., and Pourbabaee, A. (2015). "Effects of rice husk biochar application on the properties of alkaline soil and lentil growth," *Plant Soil Environ.* 61, 475-482. DOI: 10.17221/117/2015-PSE

Adedibu, P. A. (2023). *Ecological Problems of Agriculture: Impacts and Sustainable Solutions*, ScienceOpen Preprints. DOI: 10.14293/PR2199.000145.v1

Agency for toxic substances and disease registry (ATSDR). (2002). "Toxicological Profile for Aldrin/Dieldrin".

Ahmad, M., Rajapaksha, A. U., Lim, J. E., Zhang, M., Bolan, N., Mohan, D., Vithanage, M., Lee, S. S., and Ok, Y. S. (2014). "Biochar as a sorbent for contaminant management in soil and water: A review," *Chemosphere* 99, 19-33. DOI: 10.1016/j.chemosphere.2013.10.071

Ahmed, M. J., and Ahmed, Z. (2019). "Absorption of cadmium from wastewater by rice husk biochar: Adsorption equilibrium, kinetics, thermodynamics and desorption studies," *Journal of Environmental Chemical Engineering* 7(5), article 103362.

Al Moharbi, S. S., Devi, M. G., Sangeetha, B. M., and Jahan, S. (2020). "Studies on the removal of copper ions from industrial effluent by *Azadirachta indica* powder," *Appl. Water Sci.* 10, 458-466. DOI: 10.1007/s13201-019-1100-z

Amen, R., Yaseen, M., Mukhtar, A., Klemeš, J. J., Saqib, S., Ullah, S., Al-Sehemi, A. G., Rafiq, S., Babar, M., Fatt, C. L. *et al.* (2020). "Lead and cadmium removal from wastewater using eco-friendly biochar adsorbent derived from rice husk, wheat straw, and corncob," *Clean. Eng. Technol.* 1, article 100006. DOI: 10.1016/j.clet.2020.100006

Ayawei, N., Ebelegi, A. N., and Wankasi, D. (2017). "Modelling and interpretation of adsorption isotherms," *Journal of Chemistry* 2017, 1-11. DOI: 10.1155/2017/3039817

Bakkaloglu, S., Ersan, M., Karanfil, T., and Apul, O. G. (2021). "Effect of superfine pulverization of powdered activated carbon on adsorption of carbamazepine in natural source waters," *Science of the Total Environment* 793, article 148473. DOI: 10.1016/j.scitotenv.2021.148473

Bielská, L., Škulcová, L., Neuwirthová, N., Cornelissen, G., and Hale, S. E. (2018). "Sorption, bioavailability and ecotoxic effects of hydrophobic organic compounds in biochar amended soils," *Science of the Total Environment* 624, 78-86. DOI: 10.1016/j.scitotenv.2017.12.098

Cara, I. G., Țopa, D., Puiu, I., and Jităreanu, G. (2022). "Biochar a promising strategy for pesticide-contaminated soils," *Agriculture* 12(10), article 1579. DOI: 10.3390/agriculture12101579.

Chen, Y., Li, J., Li, Q., Li, Y., Li, X., Wang, Y., and Li, A. (2020). "Adsorption of multiple heavy metals from wastewater by hierarchical porous carbons derived from pomelo peels," *Journal of Hazardous Materials* 381, article 120945.

Duwiejuah, A. B. (2017). *Eco-friendly Biochars for the Adsorption of Heavy Metals from Aqueous Phase*, MPhil Thesis, University for Development Studies, Ghana, 155 pp. Retrieved from www.udsspace.uds.edu.gh.

Enaime, G., Baçaoui, A., Yaacoubi, A., and Lübken, M. (2020). "Biochar for wastewater treatment-conversion technologies and applications," *Applied Sciences (Switzerland)*, 10(10). DOI: 10.3390/app10103492

Fatombi, J. K., Osseni, S. A., Idohou, E. A., Agani, I., Neumeyer, D., Verelst, M., Mauricot, R., and Aminou, T. (2019). "Characterization and application of alkali-soluble polysaccharide of *Carica papaya* seeds for removal of indigo carmine and Congo red dyes from single and binary solutions," *Journal of Environmental Chemical Engineering* 7(5), article 103343. DOI: 10.1016/j.jece.2019.103343

Higashikawa, F. S., Conz, R. F., Colzato, M., Cerri, C. E. P., and Alleoni, L. R. F. (2016). "Effects of feedstock type and slow pyrolysis temperature in the production of biochars on the removal of cadmium and nickel from water," *J. Clean. Prod.* 137, 965-972. DOI: 10.1016/j.jclepro.2016.07.205

Hussain, S., Anjali, K. P., Hassan, S. T., and Dwivedi, P. B. (2018). "Waste tea as a novel adsorbent," *Applied Water Science* 8(6), 165. DOI: 10.1007/s13201-018-0824-5

Izah, S. C., Chakrabarty, N., and Srivastav, A. L. (2016). "A review on heavy metal concentration in potable water sources in Nigeria: Human health effects and mitigating measures," *Exposure and Health* 8, 285-304. DOI: 10.1007/s12403-016-0195-9

Kamel, F., and Hoppin. J. A. (2014). "Association of pesticide exposure with neurologic dysfunction and disease," *Environmental Health Perspectives* 112(9), 950-958. DOI: 10.1289/ehp.7135

Keçili, R., Dolak, İ., Ziyadanoğulları, B., Ersöz, A., and Say, R. (2018). "Ion imprinted cryogel-based supermacroporous traps for selective separation of cerium (III) in real samples," *Journal of Rare Earths* 36(8), 857-862. DOI: 10.1016/j.jre.2018.02.008

Li, H., Li, J., Gao, S., Li, Y., and Li, Z. (2019). "Adsorption of heavy metals from aqueous solutions by biochar derived from rice husk and corn straw under different pH conditions," *Bioresource Technology* 289, article 121677. DOI: 10.1016/j.biortech.2019.121677

Li, R., Wu, Y., Lou, X., Cheng, J., Shen, B. and Qin, L. (2023). "Porous biochar materials for sustainable water treatment: Synthesis, modification and application," *Water* 15, article 395. DOI: 10.3390/w15030395

Li, Z., Zheng, Z., Li, H., Xu, D., Li, X., Xiang, L., and Tu, S. (2023). "Review on rice husk biochar as an adsorbent for soil and water remediation," *Plants* 12, article 1524. DOI: 10.3390/plants1207152

Li, Z.; Zheng, Z., Li, H., Xu, D., Li, X., Xiang, L., and Tu, S. (2023). "Review on rice husk biochar as an adsorbent for soil and water remediation," *Plants* 12, article 1524. DOI: 10.3390/plants12071524.

Malik, D., Jain, Chakresh, Y. and Banerjee, S. (2017). "Role of plant-based biochar in pollutant removal: An overview," *Advanced Materials for Wastewater Treatment* 313-330. DOI: 10.1002/9781119407805.ch9

Mohammadi, A., Cowie, A., Mai, T. L. A., de la Rosa, R. A., Kristiansen, P., Brandao, M. and Joseph, S. (2016). "Biochar use for climate-change mitigation in rice cropping systems". *J. Clean. Prod.* 116, 61-70. DOI: 10.1016/j.jclepro.2015.12.083

Moschet, C., Wittmer, I., Simovic, J., Junghans, M., Piazzoli, A., Singer, H., Stamm, C., Leu, C., and Hollender, J. (2014). "How a complete pesticide screening changes the assessment of surface water quality," *Environmental Science and Technology* 48(10), 5423-5432. DOI: 10.1021/es500371t

Narzari, R., Bordoloi, N., Chutia, R. S., Borkotoki, B., Gogoi, N., Bora, A., Kataki, R. (2015). "Biochar: An overview on its production, properties and potential benefits," *Biol. Biotechnol. Sustain. Dev.* 1, 13-40.

Nguyen, T. B., Nguyen, V. T., Hoang, H. G., Cao, N. D. T., Nguyen, T. T., Vo, T. D. H., and Bui, X. T. (2022). "Recent development of algal biochar for contaminant remediation and energy application: A state-of-the art review," *Current Pollution Reports* 9(1), 73-89. DOI: 10.1007/s40726-022-00243-6

Paethanom, A., and Yoshikawa, K. (2012). "Influence of pyrolysis temperature on rice husk char characteristics and its tar adsorption capability," *Energies* 5, 4941-4951. DOI: 10.3390/en5124941

Park, C. M., Han, J., Chu, K. H., Al-Hamadani, Y. A., Her, N., Heo, J., and Yoon, Y. (2017). "Influence of solution pH, ionic strength, and humic acid on cadmium adsorption onto activated biochar: Experiment and modeling," *Journal of Industrial and Engineering Chemistry* 48, 186-193. DOI: 10.1016/j.jiec.2016.12.038

Rajapaksha, A. U., Vithanage, M., Ahmad, M., Seo, D. C., Cho, J.-S., Lee, S.-E., Lee, S. S., and Ok, Y. S. (2015). "Enhanced sulfamethazine removal by steam-activated invasive plant-derived biochar," *J. Hazard. Mater.* 290, 43-50. DOI: 10.1016/j.jhazmat.2015.02.046

Sadeghi Afjeh, M., Bagheri Marandi, G., and Zohuriaan-Mehr, M. J. (2020). "Nitrate removal from aqueous solutions by adsorption onto hydrogel-rice husk biochar composite," *Water Environ. Res.* 92, 934-947. DOI: 10.1002/wer.1288

Sanka, P. M., Rwiza, M. J., and Mtei, K. M. (2020). "Removal of selected heavy metal

ions from industrial wastewater using rice and corn husk biochar," *Water Air Soil Pollut*. 231, 244. DOI: 10.1007/s11270-020-04624-9

Satbaev, B., Yefremova, S., Zharmenov, A., Kablanbekov, A., Yermishin, S., Shalabaev, N., and Khen, V. (2021). "Rice husk research: From environmental pollutant to a promising source of organo-mineral raw materials," *Materials* 14(15), article 4119. DOI: 10.3390/ma14154119

Sathasivam, K., Rosemal, M. A. S., and Mas, H. (2010). "Banana trunk fibers as an efficient biosorbent for the removal of Cd(II), Cu(II), Fe(II) and Zn(II) from aqueous solutions," *J. Chilean Chem. Soc.* 2, 278-272. DOI: 10.4067/S0717-97072010000200030

Silverstein, R. M., Webster, F. X., and KiemLe, D. J. (2005). *Spectrometric Identification of Organic Compounds*, John Wiley and Sons, Hoboken, NJ, USA.

Smith, B. C. (2011). *Fundamentals of Fourier Transform Infrared Spectroscopy*, CRC Press, Boca Raton, FL, USA. DOI: 10.1201/b10777

Stuart, B. (2004). *Infrared Spectroscopy: Fundamentals and Applications*, John Wiley and Sons, Hoboken, NJ, USA.

Sun, C., Chen, T., Huang, Q., Wang, J., Lu, S., and Yan, J. (2019). "Enhanced adsorption for Pb (II) and Cd (II) of magnetic rice husk biochar by $KMnO_4$ modification," *Environ. Sci. Pollut. Res.* 26, 8902-8913. DOI: 10.1007/s11356-019-04321-z

Tay, C. C., Liew, H. H., Yong, S. K., Surif, S. and Abdul-Talib, S. (2012). "Cu^{2+} removal onto fungal derived biosorbents: Biosorption performance and the half saturation constant concentration approach," *Int. J. Res. Chem. and Environ.* 2, 138-143.

Zhang, H., Bayen, S., and Kelly, B. C. (2015). "Multi-residue analysis of legacy POPs and emerging organic contaminants in Singapore's coastal waters using gas chromatography-triple quadrupole tandem mass spectrometry," *Science of the Total Environment* 523, 219-232. DOI: 10.1016/j.scitotenv.2015.04.012

Zhang, J., Li, X., Li, Y., Li, J., Li, C., and Wang, L. (2019). "Adsorption of heavy metal ions from aqueous solutions using natural and modified adsorbents: A review," *Journal of Environmental Manag.* 242, 1-12.

Zhang, Y., Zhao, J., Jiang, Z., Shan, D., and Lu, Y. (2014). "Biosorption of Fe(II) and Mn(II) ions from aqueous solution by rice husk ash," *Bio. Med. Rese. Int.* 20, 105-117. DOI: 10.1155/2014/973095

Article submitted: October 16, 2023; Peer review completed: October 28, 2023; Revised version received and accepted: November 2, 2023; Published: November 15, 2023.
DOI: 10.15376/biores.19.1.257-275